International Journal of Engineering, Mathematical and Physical Sciences
ISSN: 2517-9934
Vol:2, No:11, 2008

Modeling and Simulation for Physical Vapor Deposition: Multiscale Model

Jürgen Geiser, Robert Röhle

Abstract**—**In this paper we present modeling and simulation for physical vapor deposition for metallic bipolar plates. In the models we discuss the application of different models to simulate the transport of chemical reactions of the gas species in the gas chamber. The so called sputter process is an extremely sensitive process to deposit thin layers to metallic plates. We have taken into account lower order models to obtain first results with respect to the gas fluxes and the kinetics in the chamber.

The model equations can be treated analytically in some circumstances and complicated multi-dimensional models are solved numerically with a software-package (UG unstructed grids, see [1]). Because of multi-scaling and multi-physical behavior of the models, we discuss adapted schemes to solve more accurate in the different domains and scales. The results are discussed with physical experiments to give a valid model for the assumed growth of thin layers.

Keywords**—**Convection-diffusion equations, multi-scale problem, physical vapor deposition, reaction equations, splitting methods.
AMS subject classifications—35K25, 35K20, 74S10, 70G65.

I. Introduction

We motivate our studying on simulating a thin film deposition process that can be done with PVD (physical vapor deposition) processes. In the last years the research on producing thin films to metallic plates has been increased. Novel deposition methods are low temperature and low pressure processes, that can be controlled by an underlying plasma, see [3], [2]. The interests on standard applications to TiN and TiC are immense but recently also deposition processes with new material classes known as MAX-phases are important. The MAX-phase are nanolayered terniar metal-carbides or -nitrids, where M is a transition metal, A is an A-group element (e.g. Al, Ga, In, Si, etc.) and X is C (carbon) or N (nitrogen). Such materials with nanolayed MAX-phase films can be used in the production of metallic bipolar plates, where the new thin film is at least noncorrosive and a metallic conductor.

We present models, that can be used to control flow and transport of gaseous species to the deposition layer, see [2] and [21].

We deal with a continuous flow model, while we assume a vacuum and diffusion dominated process. Such models can be solved with convection-diffusion equations. Further, we deal with kinetic models to understand the material fluxes in the PVD processes, see [3].

To solve the model equations we use analytical as also numerical methods to be as efficient as possible in the solver process, see [13].

To be precise, for numerical methods, we apply finite volume discretizations for the spatial terms and the backward Euler method or the Crank-Nicolson method for the time discretization.

To couple analytical and numerical solvers we apply operator splitting methods as effective coupling schemes. Such splitting methods can be seen as microscopic decoupling schemes to understand complicate mixed physical effects, e.g. flux streams of the species, reactions between the species and retardation processes. This can be helped to discuss each dominant physical effect in a separate decoupled model, see [14].

The paper is outlined as follows:

In section 2 we present our mathematical model and a possible reduced model for the further approximations. To solve our model equations we apply various analytical and numerical methods, which are presented in section 3. The decomposition methods to separate the singular and non-singular reaction systems are explained in section 4. The numerical experiments are given in section 5. In the contents, that are given in section 6, we summarize our results.

II. Mathematical Model

In the following the models are discussed in two directions of far field and near field problems:

1. Reaction-diffusion equations, see [15] (far-field problem);
2. Boltzmann-Lattice equations, see [21] (near-field problem).

The modeling is considered by the Knudsen Number (Kn), which is the ratio of the mean free path λ over the typical domain size L. For small Knudsen Numbers $Kn \approx 0.01-1.0$, we deal with a Navier-Stokes equation or with the convection-diffusion equation, see [16] and [18], whereas for large Knudsen Numbers $Kn \geq 1.0$, we deal with a Boltzmann equation, see [19].

A. Model for Small Knudsen Numbers (Far Field Model)

When gas transport is physically more complex because of combined flows in three dimensions, the fundamental equations of fluid dynamics become the starting point of the analysis. For our models with small Knudsen numbers we can assume a continuum flow and the fluid equations can be treated with a Navier-Stokes or especially with a convection-diffusion equation.

Three basic equations describe the conservation of mass, momentum and energy, that are sufficient to describe the gas transport in the reactors, see [19]:

1. Continuity: The conservation of mass requires that the net rate of the mass accumulation in a region is equal to the difference between the inflow and outflow rate.
2. Navier-Stokes: Momentum conservation requires that the net rate of momentum accumulation in a region is equal to the difference between the in and out rate of the momentum plus the sum of the forces acting on the system.
3. Energy: The rate of accumulation of internal and kinetic energy in a region is equal to the net rate of internal and kinetic energy in by convection plus the net rate of heat flow by conduction, minus the rate of work done by the fluid.

We will concentrate on the conservation of mass and assume that the energy and momentum is conserved, see [15]. Therefore the continuum flow can be described as convection-diffusion equation given as:

$$\frac{\partial}{\partial t}c + \nabla F - R_g = 0, \text{ in } \Omega \times [0,T], \quad (1)$$

$$F = -D\nabla c,$$

$$c(x,t) = c_0(x), \text{ on } \Omega, \quad (2)$$

$$c(x,t) = c_1(x,t), \text{ on } \partial\Omega \times [0,T], \quad (3)$$

where c is the molar concentration and F the flux of the species. D is the diffusivity matrix and R_g is the reaction term. The initial value is given as c_0 and we assume a Dirichlet Boundary with the function $c_1(x,t)$ sufficient smooth.

III. DISCRETIZATION METHODS

In this section, we deal with the discretisation methods that we use to discretize ODE and PDE systems.

A. Analytical Solution to the systems of ordinay differential equations of first order

The following ODE system is given :

$$\frac{dc}{dt} = A \cdot c(t) + b(t) \quad (4)$$

We assume the matrix A is constant and non-singular. Further we assume that $b(t)$ is a smooth function of t.

For the solution we obtain the method of integrating factor and a transformation to eigenvalues.

We have

$$c(t) = c_{\text{homo}}(t) + c_p(t), \quad (5)$$

where $c(t = t_0) = c_0$.

For the homogeneous part we have:

$$c_{\text{homo}}(t) = W_c \exp(\Lambda(t - t_0))\tilde{c}, \quad (6)$$

where $\tilde{c} = W_c^{-1} \cdot c_0$ and

$$\exp(\Lambda(t-t_0)) = \begin{pmatrix} \exp(\lambda_1(t-t_0)) & 0 & \dots & 0 \\ 0 & \exp(\lambda_2(t-t_0)) & \dots & 0 \\ 0 & 0 & \ddots & 0 \\ 0 & 0 & \dots & \exp(\lambda_n(t-t_0)) \end{pmatrix} \quad (7)$$

For the inhomogeneous part we have:

$$c_p(t) = W_c \cdot \exp(\Lambda(t)) u(t), \quad (8)$$

where $u(t) = \int_{t_0}^{t} \left(\exp(\Lambda(t))\right)^{-1} \cdot W_c^{-1} \cdot b(t) dt$ and the integration can be done approximately with an numerical integration method, e.g. [22].

We obtain the solution :

$$c(t) = W_c \exp(\Lambda(t-t_0)) W_c^{-1} c_0 + W_c \exp(\Lambda(t)) u(t), \quad (9)$$

where c_0 is the initial condition.

Remark 1. The solution can be used if we have non-singular matrices, or if the reactants have a successor. Otherwise we obtain fast numerical solvers.

B. Numerical Methods to ODEs

Here we introdue our numerical methods, which we apply to solve the underlying ODEs for their singular reaction matrix with $\det(A) = 0$.

We apply the following methods:

We use the implicit trapezoidal rule

$$\begin{array}{c|cc} 0 & & \\ 1 & \frac{1}{2} & \frac{1}{2} \\ \hline & \frac{1}{2} & \frac{1}{2} \end{array} \quad (10)$$

Further we use the following implicit Runge-Kutta methods: Lobatto IIIA

$$\begin{array}{c|ccc} 0 & 0 & 0 & 0 \\ \frac{1}{2} & \frac{5}{24} & \frac{1}{3} & -\frac{1}{24} \\ 1 & \frac{1}{6} & \frac{2}{3} & -\frac{1}{6} \\ \hline & \frac{1}{6} & \frac{2}{3} & -\frac{1}{6} \end{array} \quad (11)$$

Remark 2. We can also apply integration methods for the right hand side.

C. Numerical Methods to the PDEs

We consider the numerical treatment of the advection equation takes the form

$$R\phi\partial_t u + \nabla \cdot (vu) = 0, \ (t,x) \in [0,T] \times \Omega, \quad (12)$$

$$u(0,x) = U_1(0,x), \ \mathrm{x} \in \partial\Omega, \quad (13)$$

$$u(t,x) = U_2(t,x), \ (t,x) \in [0,T] \times \partial\Omega^{\text{Dirich}}, \quad (14)$$

The initial conditions are given by $U(0,x)$ and $U(t,\gamma)$ is explicitly given for $t>0$ at the inflow boundary $\gamma \in \partial^{in}\Omega$, where $\partial^{in}\Omega := \{x \in \partial\Omega,\ \mathrm{n}\cdot \mathrm{v}<0\}$. We have $\partial^{in}\Omega \cup \Omega^{\mathrm{Dirich}} = \partial\Omega$. The exact solution of (12) can be defined directly using the so called "forward tracking" form of characteristics curves. If the solution of (12) is known for some time point $t_0 \geq 0$ and for some point $y \in \Omega \cup \partial^{in}\Omega$, then u remains constant for $t \geq t_0$ along the characteristic curve $X = X(t)$ i.e., $u(t, X(t)) = u(t_0, y)$ and

$$X(t) = X(t;t_0,y) = y + \int_{t_0}^{t} \frac{v(X(s))}{R(X(s))\phi(X(s))} ds. \quad (15)$$

The characteristic curve $X(t)$ starts at time $t = t_0$ in the point y, i.e. $X(t_0;t_0,y) = y$, and it is tracked forward in time for $t > t_0$. Of course, one can obtain that $X(t) \notin \Omega$, i.e. the characteristic curve can leave the domain Ω through $\partial^{\mathrm{out}}\Omega$.

Consequently, one has that $u(t, X(t;t_0,y)) = U(t_0,y)$, where the function $U(0,y)$ is given for $t_0 = 0$ and $y \in \Omega$ by initial conditions (12) and for $t_0 > 0$ and $y \in \partial^{\mathrm{in}}\Omega$ by the inflow boundary conditions (12). The solution $u(t,x)$ of (12) can be expressed also in a "backward tracking" form that is more suitable for a direct formulation of discretization schemes. Concretely, for any characteristic curve $X = X(t) = X(t;s,Y)$ that is defined in a forward manner, i.e. $X(s;s,Y) = Y$ and $t \geq s$, one obtains the curve $Y = Y(s) = Y(s;t,x)$, which is defined in a backward manner, i.e. $Y(t;t,X) = X$ and $s \leq t$. If we express Y as function of t_0 for $t_0 \leq t$, one obtains from (15)

$$Y(t_0) = Y(t_0;t,x) = x - \int_{t_0}^{t} \frac{v(X(s))}{R(X(s))\phi(X(s))} ds \quad (16)$$

and one has $u(t,x) = u(t_0, Y(t_0))$.

To simplify our treatment of inflow boundary conditions, we suppose that $U(t,\gamma) = U^{n+1/2} \equiv \mathrm{const}$ for $\gamma \in \partial^{\mathrm{in}}\Omega$ and $t_0 \in [t^n, t^{n+1})$. Moreover, we define formally for any $\gamma \in \partial^{\mathrm{in}}\Omega$ and $t_0 \in [t^n, t^{n+1}]$ that for $t^n \leq s \leq t_0$.

In [12], the so called "flux-based (modified) method of characteristics" was described that can be viewed as an extension of standard finite volume methods (FVMs). The standard FVM for differential equation (12) takes the form

$$|\Omega_j| R_j \phi_j u_j^{n+1} = |\Omega_j| R_j \phi_j u_j^n - \sum_k \int_{t^n}^{t^{n+1}} \int_{\Gamma_{jk}} n_j(\gamma)\cdot v(\gamma) u(t,\gamma)\, d\gamma\, dt, \quad (17)$$

The idea of flux-based method of characteristics is to apply the substitution $u(t,\gamma) = u(t^n, Y(t^n;t,\gamma))$ in (17).

Particularly, for the integration variable $t \in (t^n, t^{n+1})$ and for each point $\gamma \in \partial^{\mathrm{out}}\Omega_j$, the characteristic curves $Y(s)$ are tracked backward starting in at $s = t$ and finishing in $s = t^n$. One must reach a point $Y = Y(t^n)$ such that $Y \in \partial^{\mathrm{in}}\Omega$ or $Y \in \Omega$. In the first case $u(t^n, Y)$ is given by the inflow concentration $U(t^n, Y) = U^n$, in the latter one by $u(t^n, Y)$.

The integral in right hand side of (17) can be solved exactly for the one dimensional case with general initial and boundary conditions, see e.g. [20]. For general 2D or 3D case, a numerical approximation of $u(t_0, Y(t_0))$, respectively of $Y(t_0)$, shall be used.

IV. SPLITING METHODS

In the following splitting methods of first order are described. We consider the following ordinary linear differential equations:

$$\partial_t c(t) = A\cdot c(t) + B\cdot c(t), \quad (18)$$

where the initial conditions are given as $c^n = c(t^n)$. The operators A and B are assumed to be bounded linear operators in the Banach space X with $A, B : X \to X$. In applications the operators correspond to the physical operators, e.g. the convection- and the diffusion-operator.

The operator-splitting method is introduced as a method which solves two equation parts sequentially, with respect to initial conditions. The method is given as following

$$\frac{\partial c^*(t)}{\partial t} = A\cdot c^*(t), \text{ with } c^*(t^n) = c^n \quad (19)$$

$$\frac{\partial c^{**}(t)}{\partial t} = B\cdot c^{**}(t), \text{ with } c^{**}(t^n) = c^*(t^{n+1}),$$

where the time-step is given as $\tau^n = t^{n+1} - t^n$. The solution of the equation (18) is $c^{n+1} = c^{**}(t^{n+1})$.

The splitting-error of the method is derived with Taylor-expansion, cf. [10].

We obtain the global error as

$$\rho_n = \frac{1}{\tau}\left(\exp(\tau^n(A+B)) - \exp(\tau^n B)\exp(\tau^n A)\right)c(t^n)$$

$$\frac{1}{2}\tau^n [A,B] c(t^n) + O\left((\tau^n)^2\right), \quad (20)$$

where $[A,B] = AB - BA$ is the commutator of A and B. We get an error $O(t^n)$ if the operators A and B do not commute, otherwise the method is exact.

A. Splitting with respect to the numerical and analytical methods

Here we present a splitting method with respect to the numerical and analytical methods for the differential equations. Often an analytical method can be used to solve more efficient parts of the full equation system, see [10]. The other parts can be solved more efficiently by numerical methods.

In our following example we split a system of ODEs with respect to an analytical method (transformation to an eigenvalue problem) and a numerical method (Trapeziodal rule).
We deal with the following system of ODEs:

$$\frac{dc}{dt} = M \cdot c, \tag{21}$$

$$c(0) = c_0, \tag{22}$$

where $c = c(c_1, \ldots, c_n)'$ is the solution vector of the ODE system.
The reaction matrix M is given as:

$$M = M_1 + M_2, \tag{23}$$

where M is the full matrix of the ODE system and M_1 is the part of the analytical method, where M_2 is the part of the numerical method.

So $\det(M_1) \neq 0$ and $\det(M_1) \neq 0$, which means for the M_1 matrix we can obtain a transformation to an eigenvalue equation, where for M_2 we can not use the transformation to an eigenvalue problem and apply the numerical methods.
Our algorithm is given as:

Algorithm 1

1.) Split the reaction matrix M : M_1 : Matrix with non zero eigenvalues, M_2 : Matrix with zero eigenvalues
2.) Compute the equation part

$$\frac{d\tilde{c}}{dt} = M_1 \cdot \tilde{c}, \tag{24}$$

$$\tilde{c}(0) = \tilde{c}_0 \tag{25}$$

with the analytical method, see section 3.
3.) Compute the equation part

$$\frac{d\hat{c}}{dt} = M_2 \cdot \hat{c}, \tag{26}$$

$$\hat{c}(0) = \hat{c}_0 \tag{27}$$

with the numerical method, see section 3.
4.) The result is given as: $c = (\tilde{c}, \hat{c})$.

V. EXPERIMENT FOR THE SPUTTER PROCESS

In the following section we present the various sputter processes and discuss the numerical experiments.

A. Sputter Reactions

In the following experiments we discuss the reaction models of the sputter process.

i) Experiment 1: High Energy Level

In this model one assumes a high energy level for the sputtering process, based on the work of [3].
We deal with the following reaction scheme:

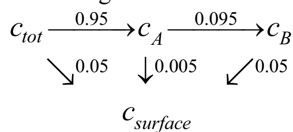

The initial conditions are given with $c_{tot,0} = 1.0$, $c_{A,0} = c_{B,0} = c_{\text{surface},0} = 0$ and we can deal with the following reaction equations:

$$\frac{dc_{tot}}{dt} = -c_{tot}, \tag{28}$$

$$\frac{dc_A}{dt} = 0.95c_{tot} - 0.1c_A, \tag{29}$$

$$\frac{dc_B}{dt} = 0.095c_A - 0.05c_B, \tag{30}$$

$$\frac{dc_{\text{surface}}}{dt} = 0.05c_{tot} + 0.005c_A + 0.05c_B, \tag{31}$$

where the total particle density is given as c_{tot}, the single particles are given as c_A and c_B and the surface particle density is given as c_{surface}.

As a result of the computation we show the Fig. 1. Additionally we present the hysteresis of c_A and c_{surface} in Fig. 2.

Remark 3. The model can be used to have an overview to horizontal gas flows across the thin layer. We can compute the growth rate depending on the amount of the velocity and diffusion. The simulations are done with Maple and Mathematica.

ii) Experiment 2: Low Energy Sputtering

In the next experiment we deal with a lower energy level and assume the resting of the molecules to a later time at the target layer. For the low energy sputtering we assume a reaction scheme given in [3]:

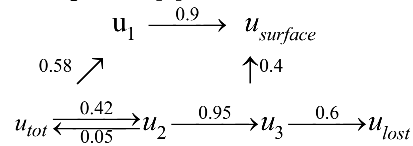

The initial conditions are given with $u_{tot,0} = 1.0$ and $u_{1,0} = u_{2,0} = u_{3,0} = u_{\text{surface},0} = u_{\text{lost},0} = 0$ and we can deal with the following reaction equations:

$$\frac{du_{tot}}{dt} = -u_{tot} + 0.05u_2, \tag{32}$$

$$\frac{du_1}{dt} = 0.58u_{tot} - 0.9u_1, \tag{33}$$

$$\frac{du_2}{dt} = 0.42u_{tot} - u_2, \tag{34}$$

$$\frac{du_3}{dt} = 0.95u_2 - u_3, \tag{35}$$

$$\frac{du_{\text{surface}}}{dt} = 0.9u_1 + 0.4u_3, \tag{36}$$

$$\frac{du_{\text{lost}}}{dt} = 0.6u_3. \tag{37}$$

As a result of the computation we get the graphs shown in Fig. 3. We present the hysteresis of u_1 and u_3 in Fig. 4.

iii) Experiment 3: Energy level with precursor gas or offsets

In this model one assumes an energy level and a precursor gas for the sputtering process, based on the work of [3].
In this experiment we deal with the following reaction:

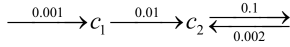

The initial conditions are given with $c_{1,0} = 1.0,\ c_{2,0} = 0.1$ and we deal with the following reaction equations:

$$\frac{dc_1}{dt} = -0.01 c_1 + 0.001, \tag{38}$$

$$\frac{dc_2}{dt} = 0.01 c_1 - 0.1 c_2 + 0.001. \tag{39}$$

As a result of the computation we get the graphs shown in the Fig. 5 and 6.
By changing the reaction coefficients we get the following reaction:

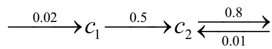

The initial conditions are given with $c_{1,0} = 1.0,\ c_{2,0} = 0.1$ and we get the following reaction equations:

$$\frac{dc_1}{dt} = -0.5 c_1 + 0.02, \tag{40}$$

$$\frac{dc_2}{dt} = 0.5 c_1 - 0.8 c_2 + 0.02. \tag{41}$$

As a result of the computation we get the graphs shown in Fig. 7.
Remark 4. In the model we assume a homogeneous and inhomogeneous reaction. Because of the small offset of the inhomogeneous reaction, we nearly obtain the same results.

iv) Experiment 4: Energy level with precursor gas and linear offsets

In this model one assumes an energy level and a precursor gas for the sputtering process, based on the work of [3]. Here we have a linear offset for the precursorn gases.
We can also analyze a variation of this reaction where we have an time dependent inhomogenous part. The reaction is then given with:

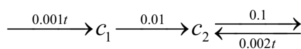

The initial conditions are given with $c_{1,0} = 1.0,\ c_{2,0} = 0.1$ and we can deal with the following reaction equations:

$$\frac{dc_1}{dt} = -0.01 c_1 + 0.001 t, \tag{42}$$

$$\frac{dc_2}{dt} = 0.01 c_1 - 0.1 c_2 + 0.002 t. \tag{43}$$

As a result of the computation we get the graphs shown in Fig. 8.
Remark 5. In the model we assume a homogeneous and inhomogeneous reaction. Because of the small offset of the inhomogeneous reaction, we nearly obtain the same results.

B. Reactive Sputtering Process

A simple model of reactive sputtering given by [?] can describe the understanding of the hysteresis and other properties of the reactive sputtering deposition.
We have the following equations:

$$n_{\text{target}} \partial_t \theta_{\text{target}} = i \Gamma_r s_r \left(1 - \theta_{\text{target}}\right) - \Gamma_i \gamma_c \theta_{\text{target}} + \Gamma_i \gamma_m \theta_{\text{substrate}},\ \mathrm{t} \in (0, T), \tag{44}$$

$$n_{\text{subsrate}} \partial_t \theta_{\text{substrate}} = i \Gamma_r s_r \left(1 - \theta_{\text{substrate}}\right) + \Gamma_i \gamma_c \theta_{\text{target}} \frac{A_t}{A_s} - \Gamma_i \gamma_m \theta_{\text{substrate}} \frac{A_t}{A_s},\ \mathrm{t} \in (0, T), \tag{45}$$

$$\partial_t N_r = \Gamma_r s_r \left(\left(1 - \theta_{\text{target}}\right) A_t + \left(1 - \theta_{\text{substrate}}\right) A_s \right), \tag{46}$$

$$\Gamma_{sput} = \Gamma_i \left(\gamma_m \theta_{\text{substrate}} + \gamma_c \theta_{\text{target}} \right), \tag{47}$$

where θ_{target} and $\theta_{\text{substrate}}$ are the fraction of the target and substrate areas, which is covered by the compound film. γ_m and γ_c are the yields for sputtering the metal and the compound from the target.

We have Γ_i and Γ_r the incident ion and reactive gas molecule fluxes. s_r is the sticking coefficient of a reactive molecule on the metal part of the target. Further A_t and A_s are the target and the substrate areas. The total number of reactive gas molecules per second that are consumed to form the compound deposited on the substrate is N_r. The target sputtering flux is Γ_{sput}
For our experiments we use the following parameters, while we variate the parameters $\Gamma_r s_r,\ \Gamma_i \gamma c,\ \Gamma_i \gamma_m$.

$$n_t = n_s = 1,$$
$$i = 1,$$
$$A_t = 0.25,$$
$$A_s = 0.75,$$

where the starting conditions are given with $\theta_{\text{target},0} = 1.0$ and $\theta_{\text{substrate},0} = 0.1$.

i) First Experiment:

In our first experiment the variable parameters are given with:

$$\Gamma_r s_r = 0.1,$$
$$\Gamma_i \gamma_c = 0.07,$$
$$\Gamma_i \gamma_m = 0.05.$$

We get the following simplified system of ODEs:

$$\partial_t \theta_{\text{target}} = -0.17 \cdot \theta_{\text{target}} + 0.05 \cdot \theta_{\text{substrate}} + 0.1, \tag{48}$$

$$\partial_t \theta_{\text{substrate}} = \frac{0.07}{3} \cdot \theta_{\text{target}} - \frac{0.35}{3} \cdot \theta_{\text{substrate}} + 0.1, \tag{49}$$

$$\partial_t N_r = -0.025 \cdot \theta_{\text{target}} - 0.075 \cdot \theta_{\text{substrate}} + 0.1, \tag{50}$$

$$\Gamma_{\text{sput}} = 0.07 \cdot \theta_{\text{target}} + 0.05 \cdot \theta_{\text{substrate}},\ \mathrm{t} \in (0, T). \tag{51}$$

For the solving of the equations we apply the eigenvalue transformation. For solving the coupled equations we apply our algorithm 1.

We present the hysterisises of θ_{target} with $\theta_{\text{substrate}}$, $\partial_t N_r$ with Γ_{sput} and N_r with Γ_{sput} in the Fig. 9, 10 and 11.

ii) Second Experiment:

In our second experiment the variable parameters are given with:

$$\Gamma_r s_r = 0.05,$$
$$\Gamma_i \gamma_c = 0.02,$$
$$\Gamma_i \gamma_m = 0.1.$$

We get the following simplified system of ODEs:

$$\partial_t \theta_{\text{target}} = -0.07 \cdot \theta_{\text{target}} + 0.1 \cdot \theta_{\text{substrate}} + 0.05, \tag{52}$$

$$\partial_t \theta_{\text{substrate}} = \frac{0.02}{3} \cdot \theta_{\text{target}} - \frac{0.35}{3} \cdot \theta_{\text{substrate}} + 0.05, \tag{53}$$

$$\partial_t N_r = -0.0125 \cdot \theta_{\text{target}} - 0.0375 \cdot \theta_{\text{substrate}} + 0.05, \tag{54}$$

$$\Gamma_{\text{sput}} = 0.02 \cdot \theta_{\text{target}} + 0.1 \cdot \theta_{\text{substrate}}, \ t \in (0, T). \tag{55}$$

For the solving of the equations we apply the eigenvalue transformation. For solving the coupled equations we apply our algorithm 1.

We present the hysterisises of θ_{target} with $\theta_{\text{substrate}}$, $\partial_t N_r$ with Γ_{sput} and N_r with Γ_{sput} in the Fig. 12, 13 and 14.

iii) Third Experiment:

In our third experiment the variable parameters are given with:

$$\Gamma_r s_r = 0.05,$$
$$\Gamma_i \gamma_c = 0.1,$$
$$\Gamma_i \gamma_m = 0.02.$$

We get the following simplified system of ODEs:

$$\partial_t \theta_{\text{target}} = -0.15 \cdot \theta_{\text{target}} + 0.02 \cdot \theta_{\text{substrate}} + 0.05, \tag{56}$$

$$\partial_t \theta_{\text{substrate}} = \frac{0.1}{3} \cdot \theta_{\text{target}} - \frac{0.17}{3} \cdot \theta_{\text{substrate}} + 0.05, \tag{57}$$

$$\partial_t N_r = -0.0125 \cdot \theta_{\text{target}} - 0.0375 \cdot \theta_{\text{substrate}} + 0.05, \tag{58}$$

$$\Gamma_{\text{sput}} = 0.1 \cdot \theta_{\text{target}} + 0.02 \cdot \theta_{\text{substrate}}, \ t \in (0, T). \tag{59}$$

For the solving of the equations we apply the eigenvalue transformation. For solving the coupled equations we apply our algorithm 1.

We present the hysterisises of θ_{target} with $\theta_{\text{substrate}}$, $\partial_t N_r$ with Γ_{sput} and N_r with Γ_{sput} in the Fig. 15, 16 and 17.

VI. CONCLUSIONS AND DISCUSSIONS

We present a continuous model, due to a far and near field idea for a flow field in a PVD apparatus. Based on different models we can predict the flow of the reacting chemicals on the different scales of the chemical reactor. For the mesoscopic scale model we discuss the discretization and solver methods. We contribute a coupling algorithm to mix analytical and numerical solutions in our models. Such schemes have benefits in computations and improve the accuracy.

Numerical examples are presented to discuss the influence of near-continuum regime at the thin film. The modeling of various inflow sources can describe the growth of the thin-film at the wafer. In future, we will analyze the validity of the models with physical experiments.

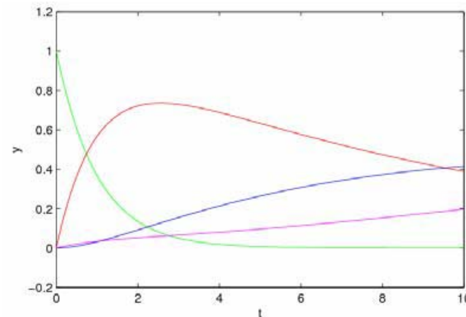

Fig. 1 1D Experiment of the heavy particle transport. green: c_{tot}, red: c_A, blue: c_B, magenta: $c_{surface}$

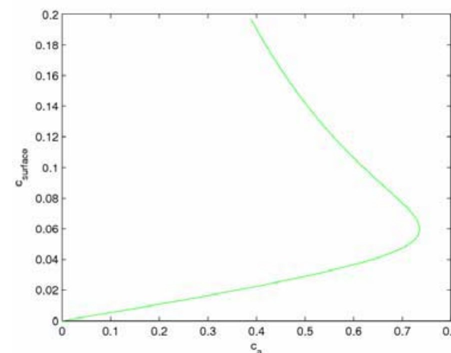

Fig. 2 Hysteresis of the concentrations c_a and $c_{surface}$

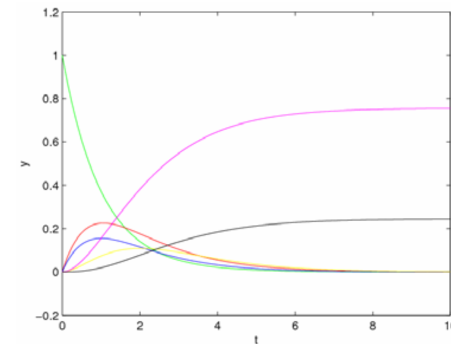

Fig. 3 1D Experiment of the heavy particle transport. green: u_{tot}, red: u_1, blue: u_2, magenta: $u_{surface}$, black: u_{lost}

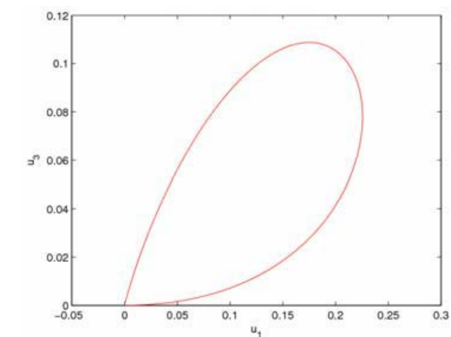

Fig. 4 Hysteresis of the concentrations u_1 and u_3

International Journal of Engineering, Mathematical and Physical Sciences
ISSN: 2517-9934
Vol:2, No:11, 2008

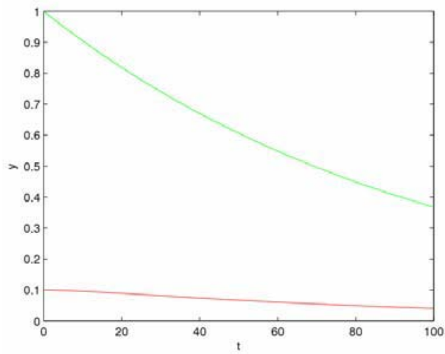

Fig. 5 1D Experiment of the heavy particle transport. green: c_1, red: c_2

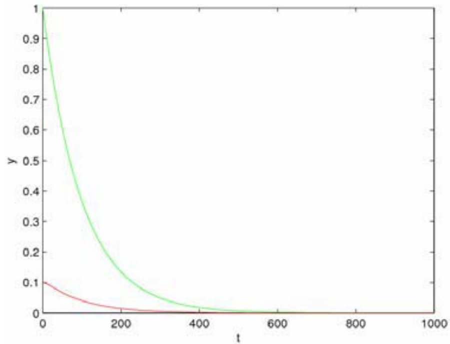

Fig. 6 1D Experiment of the heavy particle transport. green: c_1, red: c_2

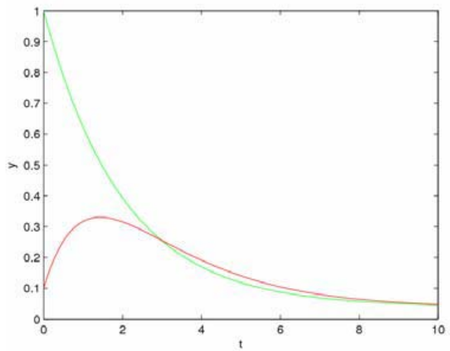

Fig. 7 1D Experiment of the heavy particle transport. green: c_1, red: c_2

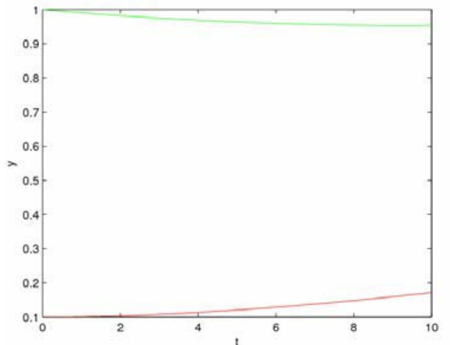

Fig. 8 1D experiment of the heavy particle transport. green: c_1, red: c_2

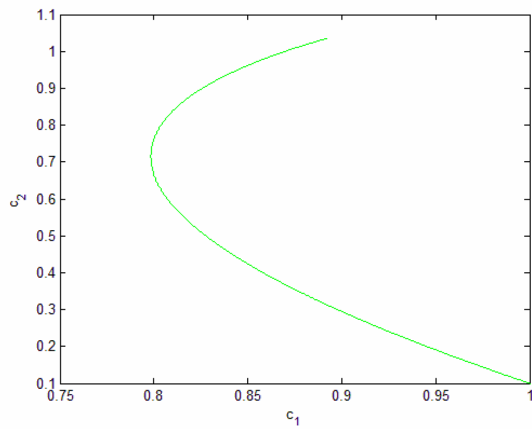

Fig. 9 First experiment: hysteresis of θ_{target} (c_1) with $\theta_{\text{substrate}}$ (c_2)

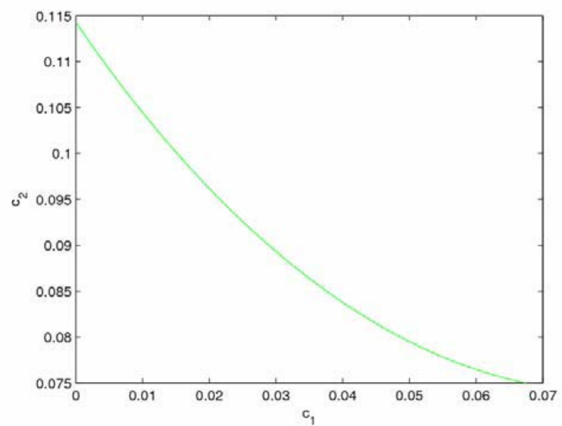

Fig. 10 First xperiment: hysteresis of $\partial_t N_r$ (c_1) with Γ_{sput} (c_2)

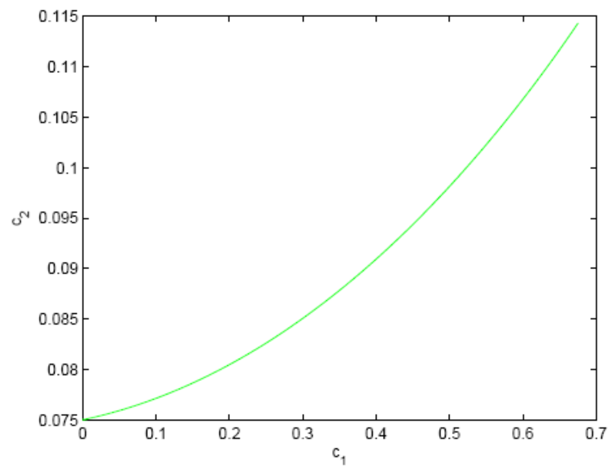

Fig. 11 First experiment: hysteresis of N_r (c_1) with Γ_{sput} (c_2)

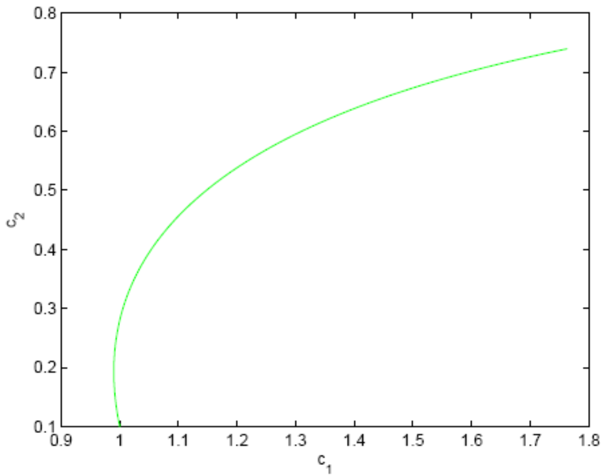

Fig. 12 Second experiment: hysteresis of θ_{target} (c_1) with $\theta_{\text{substrate}}$ (c_2)

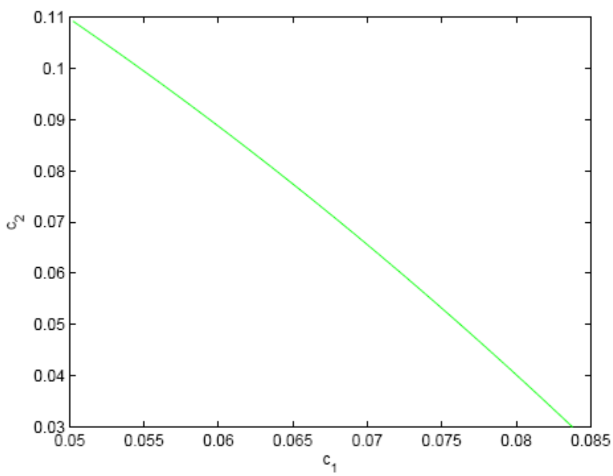

Fig. 13 Second experiment: hysteresis of $\partial_t N_r$ (c_1) with Γ_{sput} (c_2)

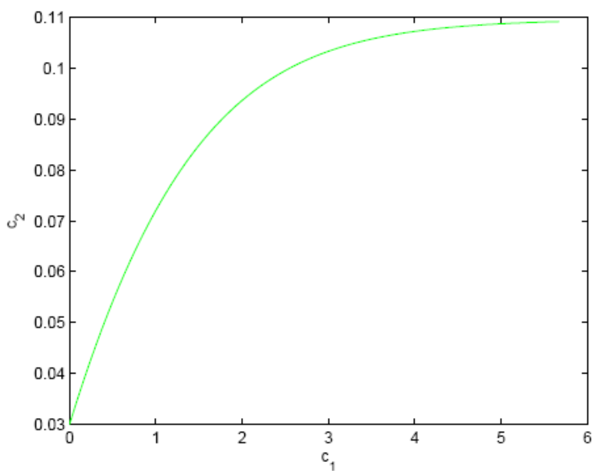

Fig. 14 Second experiment: hysteresis of N_r (c_1) with Γ_{sput} (c_2)

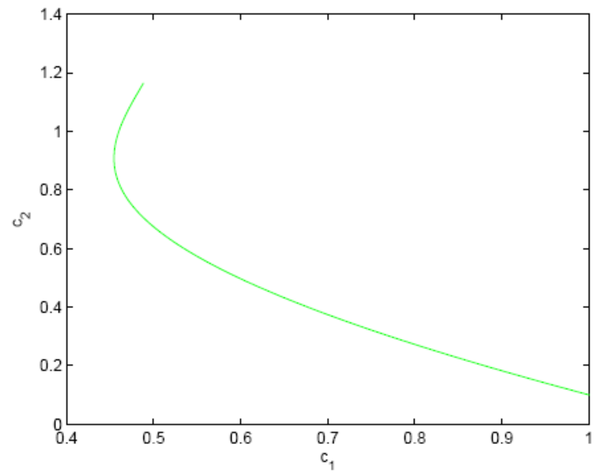

Fig. 15 Third experiment: hysteresis of θ_{target} (c_1) with $\theta_{\text{substrate}}$ (c_2)

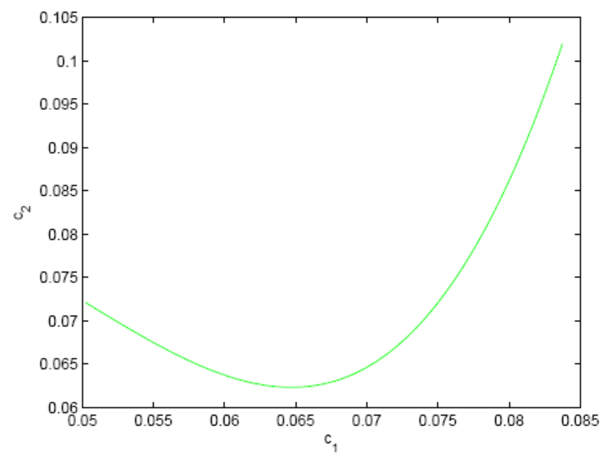

Fig. 16 Third experiment: hysteresis of $\partial_t N_r$ (c1) with Γ_{sput} (c_2)

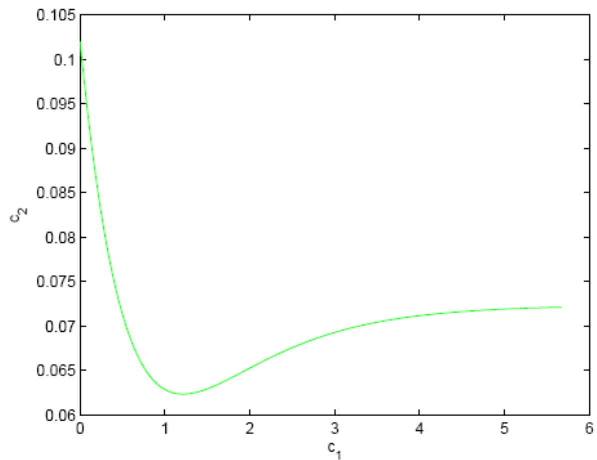

Fig. 17 Third experiment: hysteresis of N_r (c_1) with Γ_{sput} (c_2)

REFERENCES

[1] P. Bastian, K. Birken, K. Eckstein, K. Johannsen, S. Lang, N. Neuss, and H. Rentz-Reichert. UG - a flexible software toolbox for solving partial differential equations. Computing and Visualization in Science, 1(1):27–40, 1997.

[2] S. Berg and T. Nyberg. Fundamental understanding and modeling of reactive sputtering processes. Thin Solid Films, 476, 215-230, 2005.

[3] D.J. Christie. Target material pathways model for high power pulsed magnetron sputtering. J.Vac.Sci. Technology, 23:2, 330-335, 2005.

[4] P. Csomos, I. Farago and A. Havasi. Weighted sequential splittings and their analysis. Comput. Math. Appl., (to appear)

[5] K.-J. Engel, R. Nagel, One-Parameter Semigroups for Linear Evolution Equations. Springer, New York, 2000.

[6] I. Farago, and Agnes Havasi. On the convergence and local splitting error of different splitting schemes. E¨otv¨os Lorand University, Budapest, 2004.

[7] I. Farago. Splitting methods for abstract Cauchy problems. Lect. Notes Comp.Sci. 3401, Springer Verlag, Berlin, 2005, pp. 35-45

[8] I. Farago, J. Geiser. Iterative Operator-Splitting methods for Linear Problems. Preprint No. 1043 of theWeierstrass Institute for Applied Analysis and Stochastics, Berlin, Germany, June 2005.

[9] J. Geiser. Numerical Simulation of a Model for Transport and Reaction of Radionuclides. Proceedings of the Large Scale Scientific Computations of Engineering and Environmental Problems, Sozopol, Bulgaria, 2001.

[10] J. Geiser. Gekoppelte Diskretisierungsverfahren f¨ur Systeme von Konvektions-Dispersions-Diffusions-Reaktionsgleichungen. Doktor-Arbeit, Universität Heidelberg, 2003.

[11] J. Geiser. Discretization methods with analytical solutions for convection-diffusiondispersion-reaction-equations and applications. Journal of Engineering Mathematics, published online, Oktober 2006.

[12] J. Geiser. Discretisation and Solver Methods with Analytical Methods for Advection-Diffusion-reaction Equations and 2D Applications. Journal of Porous Media, Begell House Inc., Redding, USA, accepted March, 2008.

[13] J. Geiser. Iterative Operator-Splitting Methods with higher order Time-Integration Methods and Applications for Parabolic Partial Differential Equations. Journal of Computational and Applied Mathematics, Elsevier, Amsterdam, The Netherlands, 217, 227-242, 2008.

[14] J. Geiser. Decomposition Methods for Partial Differential Equations: Theory and Applications in Multiphysics Problems. Habilitation Thesis, Humboldt University of Berlin, Germany, under review, July 2008.

[15] M.K. Gobbert and C.A. Ringhofer. An asymptotic analysis for a model of chemical vapor deposition on a microstructured surface. SIAM Journal on Applied Mathematics, 58, 737–752, 1998.

[16] H.H. Lee. Fundamentals of Microelectronics Processing McGraw-Hill, New York, 1990.

[17] Chr. Lubich. A variational splitting integrator for quantum molecular dynamics. Report, 2003.

[18] S. Middleman and A.K. Hochberg. Process Engineering Analysis in Semiconductor Device Fabrication McGraw-Hill, New York, 1993.

[19] M. Ohring. Materials Science of Thin Films. Academic Press, San Diego, New York, Boston, London, Second edition, 2002.

[20] P.J. Roache. A flux-based modified method of characteristics. Int. J. Numer. Methods Fluids, 12:12591275, 1992.

[21] T.K. Senega and R.P. Brinkmann. A multi-component transport model for nonequilibrium low-temperature low-pressure plasmas. J. Phys. D: Appl.Phys., 39, 1606–1618, 2006.

[22] J. Stoer and R. Burlisch. Introduction to numerical analysis. Springer verlag, New York, 1993.